*Progress In Electromagnetics Research Letters, Vol. 51, 15–20, 2015*

# A Dual-Polarized MIMO Antenna with EBG for 5.8 GHz WLAN Application

**Xiaoyan Zhang[1, 2, *], Xinxing Zhong[1], Bincheng Li[3], and Yiqiang Yu[1, 2]**

**Abstract**—A dual-polarized multiple-input-multiple-output (MIMO) antenna integrated with electromagnetic band-gap (EBG) is proposed. The MIMO antenna consists of two dual-polarized (0° and 90° polarizations) antenna elements. Each element includes four symmetrical arc-shaped slots. A mushroom-shaped EBG structure with four slots at its fringe is designed to enhance the gain of MIMO antenna. The bandwidth (return loss $>$ 10 dB) of the proposed antenna is from 5.70 to 5.93 GHz, and the peak gain is 5.45 dBi. The isolation between the ports of adjacent antenna elements can be as small as less than $-20$ dB. The dual-polarized MIMO antenna with EBG has a compact volume of $44.5 \times 77.5 \times 1.6\,\text{mm}^3$ and can be suitable for 5.8 GHz WLAN application.

## 1. INTRODUCTION

As the variety and sophistication of data-intensive wireless service grows explosively, bandwidth-efficient communication techniques, as polarization diversity and MIMO technology, have gained great interest [1]. Dual-polarized antenna is superior over the mono-polarized one. It can overcome multipath effects and transmit twice more information in wireless communication. Several dual-band dual-polarized microstrip antennas are proposed in [2–4]. The patch elements were excited by two probes or two microstrip lines, and achieved $\pm 45°$ or $\pm 90°$ polarizations. Multiple-input multiple-output (MIMO) technology, which is the key technology for the fourth generation mobile communication system (4G), has potential of increasing capacity without sacrificing additional spectrum. Several MIMO antennas have been applied proposed in [5–7], and good performance has been achieved. Recently, metamaterial-based EBG has been investigated to improve antenna design, i.e., reduce antenna size, suppress surface waves [8–11], and eliminate mutual coupling between antenna's elements [12, 13].

In this paper a dual-polarized MIMO antenna with EBG is presented. In Section 2, we propose a dual-polarized antenna with two probe feeds and four symmetrical arc-shaped slots etched on the patch surface. In Section 3, a mushroom-like EBG structure with four slots at fringe of each EBG unit is designed. Moreover, a MIMO antenna with EBG is presented on the basis of the front in Section 4, and a conclusion is given in Section 5.

## 2. DUAL-POLARIZED ANTENNA DESIGN

The configuration of a dual-polarized antenna proposed for the MIMO system is illustrated in Figure 1. The proposed dual-polarized square microstrip antenna is designed on an FR-4 substrate with a thickness of 1.6 mm and a loss tangent of 0.022. It has four symmetrical arc-shaped slots in parallel with the patch's central lines on the top and a ground on the bottom. The square radiating patch has a side length of $L_1$. Each arc slot is a quadrant, and the inner and outer radii are $R_1$ and $R_2$, respectively. The spacing between two adjacent arc-shaped slots is denoted as $D$. The antenna is orthogonally excited by coaxial cable with an SMA connectors distributed in $x$ and $y$ axis, respectively. They are located

*Received 21 November 2014, Accepted 18 December 2014, Scheduled 26 December 2014*

* Corresponding author: Xiaoyan Zhang (xy_zhang3129@ecjtu.jx.cn).

[1] School of Information Engineering, East China Jiaotong University, Nanchang 330013, China. [2] The State Key Laboratory of Millimeter Wave, Nanjing, China. [3] The Institute of Optics and Electronics, The Chinese Academy of Sciences, China

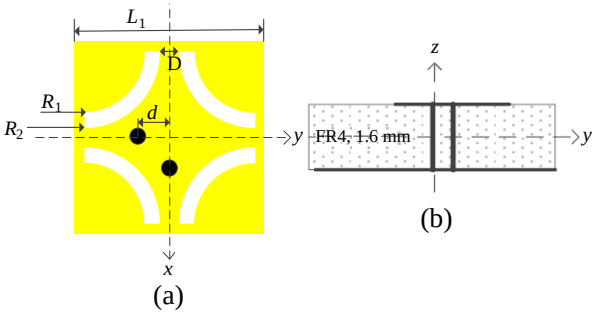


**Figure 1.** Configuration of dual-polarized antenna. (a) Front view and (b) side view.

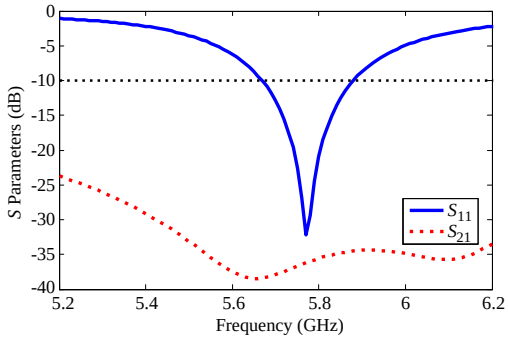


**Figure 2.** Simulated $S_{11}$ and $S_{21}$ for the dual-polarized antenna.

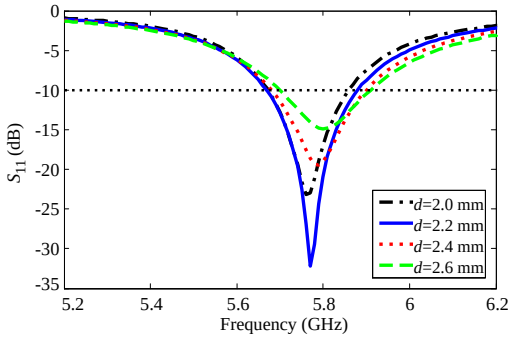


**Figure 3.** Simulated $S_{11}$ as a function of the distance $d$ between the feed point and the center of the dual-polarized antenna.

**Table 1.** Optimized geometric parameters for the dual-polarized antenna. (Unit: millimeter).

| $L_1$ | $R_1$ | $R_2$ | $D$ | $d$ |
|---|---|---|---|---|
| 11.0 | 3.0 | 3.5 | 2.0 | 2.2 |

at a distance of $d$ away from the patch center. This feed arrangement excites 0° ($x$-directed) and 90° ($y$-directed) linearly polarized waves at the same time. Due to the perturbation of the arc-shaped slots, the excited patch surface current paths are meandered, which results in the decrease for the operating frequencies. In other words, the size of the antenna can be reduced at a fixed operating frequency.

The dual-polarized antenna was optimized with HFSS 13.0. All the optimized geometric parameters for the dual-polarized antenna are listed in Table 1, and the size of substrate is $44.5 \times 44.5\,\text{mm}^2$. Figure 2 shows the simulated $S_{11}$ and $S_{21}$ results. It can be seen that a resonant mode generates at 5.77 GHz, covering the band from 5.67 GHz to 5.88 GHz and has an isolation of better than 34.5 dB across the obtained impedance bandwidth, which may be suitable for 5.8 GHz WLAN application.

The simulated results of $S_{11}$ with the distance $d$ varying from 2.0 to 2.6 mm are shown in Figure 3. Some effects on resonant frequency are seen that the value of $S_{11}$ increased whatever the distance $d$ increases or decreases because of the variation of impedance matching.

## 3. EBG STRUCTURE DESIGN

The electromagnetic band-gap (EBG) structures are periodical cells composed of metallic or dielectric elements. One of the most important benefits of EBG structure is to prohibit the propagation of surface wave to enhance the gain of the proposed antenna. In this paper, we design an EBG unit with four slots and one conductive via in Figure 4(b) on the basis of traditional mushroom-like EBG. The geometry

for the designed EBG structure is illustrated in Figure 4(a). All the detailed geometric parameters for the EBG structure are listed in Table 2, and $g$ is the gap between two units.

There are different ways to investigate whether or not a periodic structure acts as an EBG in the desired frequency range. In this paper, the truncated periodic structures are placed in ideal TEM

**Table 2.** Optimized parameters for the EBG structure. (Unit: millimeter).

| $a$ | $r$ | $L$ | $g$ |
|---|---|---|---|
| 5 | 0.3 | 3.5 | 0.5 |

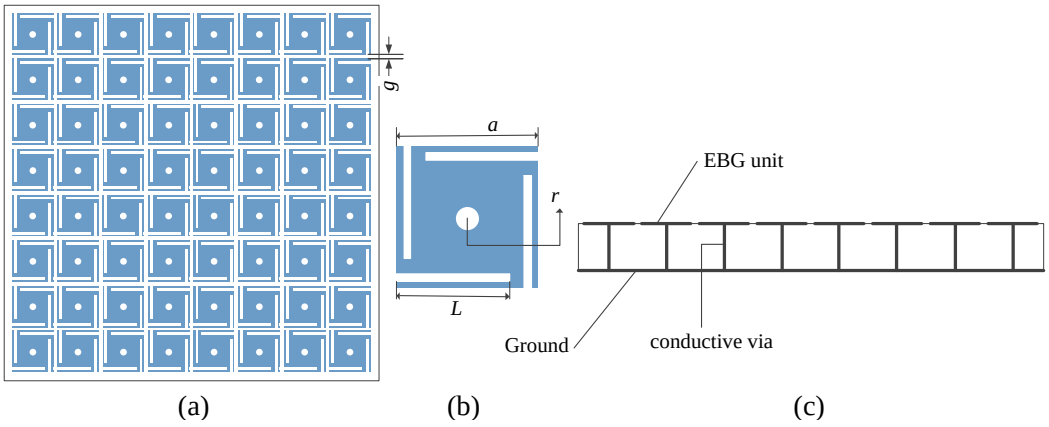


**Figure 4.** Geometry for the EBG structure. (a) $8 \times 8$ EBG structure, (b) EBG unit, and (c) side view.

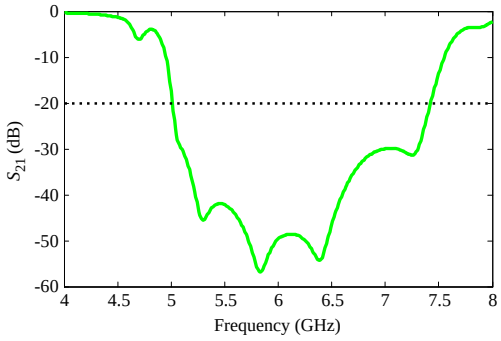


**Figure 5.** $S_{21}$ for the $8 \times 8$ EBG units.

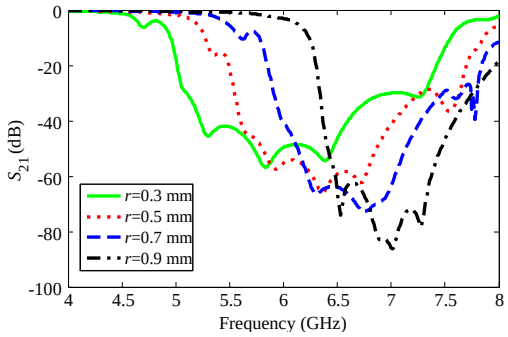


**Figure 6.** Simulated $S_{21}$ as a function of radius of conductive via.

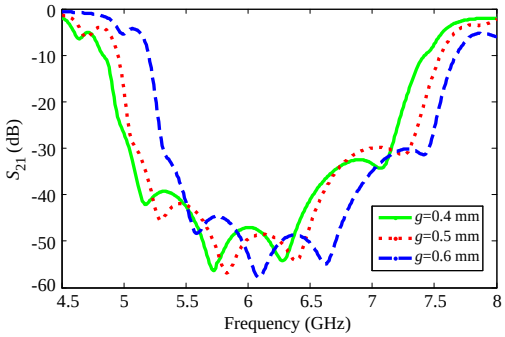


**Figure 7.** Simulated $S_{21}$ as a function of the gap between two units.

waveguides [11]. The detailed simulation model consists of a two-port waveguide formed by a pair of perfect electric conductor (PEC) along the $z$ direction and perfect magnetic conductor (PMC) along the $x$ direction. The input wave is launched in free space toward the inside of waveguide at normal incidence from each port. It can form a TEM waveguide with this boundary condition. $8 \times 8$ EBG units are centered in the waveguide along the $y$ direction. In this configuration, the magnitude of $S$ parameters is simulated and shown in Figure 5. There is a band-gap between the frequencies 5.02 GHz–7.42 GHz with a criteria of $-20$ dB, in which the electromagnetic wave cannot propagate, due to the high surface impedance of EBG structure within the band-gap.

For the purpose of optimized performance, the studies of parameters of the antenna structure are carried out. First, we analyze the radius ($r$) of conductive via. As presented in Figure 6, the band-gap of EBG structure is changeable. The band-gap moves to higher frequency and $S_{21}$ becomes obviously smaller when the radius gets larger. This is because the conductive via acts as equivalent inductance, according to formula $f_0 = \frac{1}{2\pi\sqrt{LC}}$, where $f_0$ is resonant frequency, and $L$ and $C$ are represent equivalent inductance and capacitance respectively. Therefore, as the radius of the conductive via gets larger, the equivalent inductance gets smaller, and the resonant frequency which is the center $s$ frequency of the band-gap gets higher.

The band-gap is also affected by the gap between two units. As shown in Figure 7, the gap is changed from 0.3 mm to 0.9 mm. The wider the gap is, the higher of the resonant frequency, and the narrower bandwidth will be. This is attributable to the variation of the equivalent capacitance. The gap can be equivalent to capacitance. As the gap becomes wider, the equivalent capacitance becomes smaller, so the band-gap will move to higher frequency.

## 4. DUAL-POLARIZED MIMO ANTENNA WITH EBG

The dual-polarized antenna element and the EBG structure designed in previous sections are employed to develop a two-element MIMO system. The configuration of the two-element MIMO antenna system is depicted in Figure 8. Two dual-polarized antennas are surrounded by the EBG structure, and four feeds are separately marked as 1, 2, 3, and 4, representing ports 1, 2, 3, and 4 respectively. All the dimensions of the antenna and EBG structure are the same as in those in the previous sections. A photo of the fabricated antenna is shown in Figure 9. To test the proposed antenna, four 50 coaxial cable with SMA connectors are soldered on the back side of the FR-4 substrate.

The simulated and measured $S_{11}$ with and without EBG are plotted in Figure 10. It can be observed that the antennas without EBG resonate at 5.76 GHz, and have a bandwidth from 5.67 to 5.87 GHz and a return loss of less than $-10$ dB. The antennas with EBG generates a resonant mode at 5.81 GHz covering 5.70–5.93 GHz band compared with the resonant mode at 5.79 GHz by simulation. Agreement between the simulation and measurement can be found from the results. The resonant frequency of antennas with EBG becomes slightly higher due to the coupling between the antenna elements and EBG structure.

Figure 11 shows the measured far fields radiation patterns for the dual-polarized MIMO antenna with EBG at 5.81 GHz. It can be seen that the peak gain at resonant frequency is about 5.45 dBi. In order to demonstrate the function of the EBG, a comparison result of peak gain at different frequencies

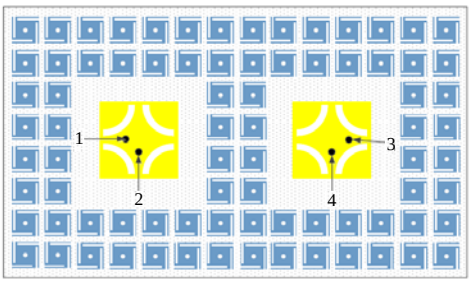


**Figure 8.** Prototype of dual-polarized MIMO antenna with EBG.

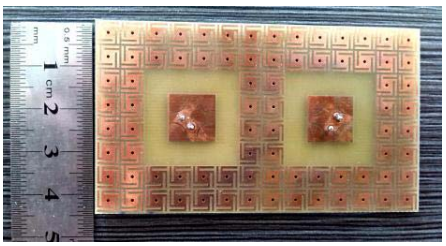

**Figure 9.** Photo of the fabricated antenna.

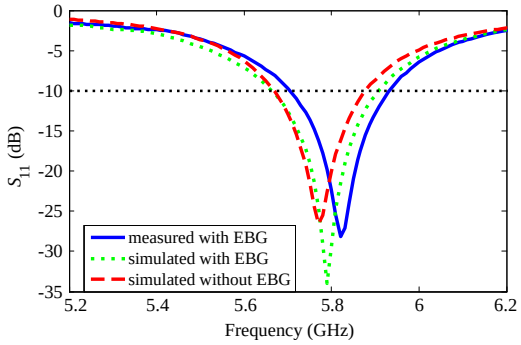


**Figure 10.** Simulated and measured $S$-parameters of dual-polarized MIMO antenna with EBG and without EBG.

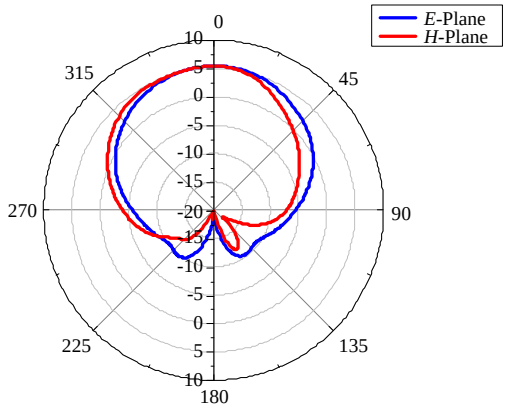


**Figure 11.** Measured far fields radiation patterns for dual-polarized MIMO antenna with EBG at 5.81 GHz.

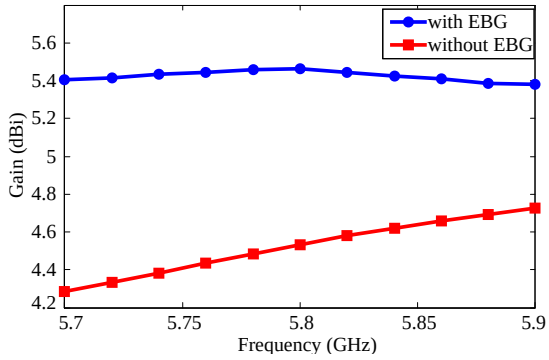


**Figure 12.** Measured peak gain of dual-polarized MIMO the antenna with EBG and without EBG.

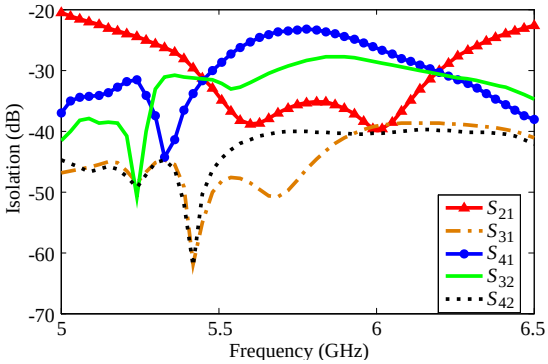


**Figure 13.** Measured isolation of port 1 and 2.

is given in Figure 12. An obviously increment of peak gain can be seen after integrated with the EBG structure.

Isolation is an important parameter for a MIMO antenna system, which can be described through $S$ parameters. Due to the system's symmetry, we need to research the isolation between port 1 or 2 and other ports. The isolation of ports 1 and 2 is plotted in Figure 13. The isolation between each port can reach $-20$ dB at least at the working band (5.725–5.825 GHz), so it can be demonstrated that this MIMO system has a good isolation.

## 5. CONCLUSION

A dual-polarized multiple-input-multiple-output (MIMO) antenna with electromagnetic band-gap (EBG) has been proposed in this paper. The entire MIMO antenna system has a compact volume of $44.5 \times 77.5 \times 1.6\,\text{mm}^3$. Each antenna is of dual-linear-polarization (0° and 90° polarizations) by using two orthorhombic feeds. Moreover, a mushroom-like EBG structure is designed surrounding the MIMO antenna. It has been demonstrated that the EBG can improve gain and directivity. The bandwidths (return loss $>$ 10 dB) achieved for the proposed dual-polarized MIMO antenna with EBG are 5.70–5.93 GHz, and it achieves peak gain of 5.46 dBi. The isolation between the ports can reach as low as $-20$ dB at least. The dual-polarized MIMO antenna with EBG studied in this paper is suitable for 5.8 GHz WLAN application.

## ACKNOWLEDGMENT

This work was supported in part by the National Natural Science Foundation of China (Nos. 61061002, 61261005), Jiangxi Provincial Department of Education Project funded (No. GJJ13352), the Open Project of State Key Laboratory of Millimeter Wave (No. K201325) and the 555 Talent Program of Jiangxi Province, all in China.

## REFERENCES

1. Serinken, N., M. Jorgenson, K. W. Moreland, S. Chow, and T. Willink, "Polarization diversity in high frequency radio data systems," *Electronics Letters*, Vol. 32, No. 19, 1824–1826, Sep. 1996.
2. Row, J. S., S. H. Yeh, and K. L. Wong, "Compact dual-polarized microstrip antennas," *Microwave and Optical Technology Letters*, Vol. 27, No. 4, 284–287, Nov. 2000.
3. Gosalia, K. and G. Lazzi, "Reduced size, dual-polarized microstrip patch antenna for wireless Communications," *IEEE Transactions on Antennas Propagation*, Vol. 51, No. 9, 2182–2186, Sep. 2003.
4. Moradi, K. and S. Nikmehr, "A dual-band dual-polarized microstrip array antenna for base stations," *Progress In Electromagnetics Research*, Vol. 123, 527–541, 2012.
5. Jensen, M. A. and J. W. Wallace, "A review of antennas and propagation for MIMO wireless communications," *IEEE Transactions on Antennas Propagation*, Vol. 52, No. 11, 2810–2824, Nov. 2004.
6. Browne, D. W., M. Manteghi, M. P. Fitz, and Y. Rahmat-Samii, "Experiments with compact antenna arrays for MIMO radio communications," *IEEE Transactions on Antennas Propagation*, Vol. 54, No. 11, 3239–3250, Nov. 2006.
7. Li, W., W. Lin, and G. Yang, "A compact MIMO antenna system design with low correlation from 1710 MHz to 2690 MHz," *Progress In Electromagnetics Research*, Vol. 144, 59–65, 2014.
8. Sievenpiper, D., L. Zhang, R. Broas, N. Alexopolous, and E. Yablonovitch, "High-impedance electromagnetic surfaces with a forbidden frequency band," *IEEE Transactions on Microwave Theory and Techniques*, Vol. 47, No. 11, 2059–2074, Nov. 1999.
9. Broas, R. F. J., D. F. Sievenpiper, and E. Yablonovitch, "A high-impedance ground plane applied to a cellphone handset geometry," *IEEE Transactions on Microwave Theory and Techniques*, Vol. 49, No. 7, 1262–1265, Jul. 2001.
10. Liang, J. and H.-Y. D. Yang, "Microstrip patch antennas on tunable electromagnetic band-gap substrates," *IEEE Transactions on Antennas Propagation*, Vol. 57, No. 6, 1612–1617, Jun. 2009.
11. Foroozesh, A. and L. Shafai, "Application of combined electric-and magnetic-conductor ground planes for antenna performance enhancement," *Canadian Journal of Electrical and Computer Engineering*, Vol. 33, No. 2, 87–98, Spring 2008.
12. Yang, F. and Y. Rahmat-Samii, "Microstrip antennas integrated with electromagnetic band-gap (EBG) structures: A low mutual coupling design for array applications," *IEEE Transactions on Antennas Propagation*, Vol. 51, No. 10, 2936–2946, Oct. 2003.
13. Islam, M. T. and M. S. Alam, "Compact EBG structure for alleviating mutual coupling between patch antenna array elements," *Progress In Electromagnetics Research*, Vol. 137, 425–438, 2013.